Cooperative Host−Guest Recognition in Crystalline Clathrates: Steric Guest Ordering by Molecular Gears

Jennifer A. Swift, Anne M. Reynolds, and Michael D. Ward*

Contribution from the Department of Chemical Engineering and Materials Science, University of Minnesota, Amundson Hall, 421 Washington Avenue SE, Minneapolis, Minnesota 55455-0132

Received August 27, 1998

Supramolecular host frameworks consisting of guanidinium (G) and 4,4′-biphenyldisulfonate (BPDS) ions include a diverse variety of aromatic guests to afford clathrates with the composition $(G)_2BPDS\cdot(guest)$. Single-crystal X-ray diffraction reveals that these materials have a bilayer architecture in which the BPDS ions serve as pillars that connect opposing two-dimensional hydrogen-bonded networks of guanidinium and sulfonate ions, resulting in the formation of galleries with one-dimensional pores occupied by the guests. The solid-state structures of clathrates derived from various monosubstituted benzene guests (C_6H_5X; X = Cl, CH_3, Br, I) and disubstituted isomers (*o*,*m*,*p*-YC_6H_5X; X, Y = Cl, CH_3, Br) reveal cooperative host−guest and guest−guest interactions that affect the observed pore structure and molecular ordering in the two-dimensional galleries. The pore heights and corresponding pore sizes decrease with the introduction of halogenated guests relative to their hydrocarbon analogues, suggesting attractive host−guest interactions between halogen atoms and the guanidinium sulfonate sheets. The two-dimensional ordering of *o*- and *m*-disubstituted benzene guests in the porous galleries can be explained by cooperative steric interactions between the guests and the conformationally flexible BPDS pillars, the latter behaving as synchronous molecular gears that relay the instructions for guest ordering from one pore to another. In some cases these steric effects produce guest ordering that appears to be less than optimal with respect to guest−guest dipolar interactions. Steric effects are particularly pronounced in the 1,4-dibromobenzene clathrate, which crystallizes in an alternative "brick" architecture with larger one-dimensional pores. These materials provide insight into the molecular recognition sequences that govern the ordering of guest molecules in clathrates, which is crucial to the design of new materials based on these systems.

Introduction

Crystalline organic clathrates[1] consisting of molecular host frameworks that encapsulate molecular guests provide a unique opportunity to study the fundamental physicochemical phenomena associated with molecular recognition and ordering. The promise of these materials in chemical separations, catalysis, optoelectronics, and magnetics has stimulated efforts to develop crystal engineering strategies for the synthesis of open host frameworks. These strategies typically rely on "programmed" assembly of host frameworks through carefully designed noncovalent interactions between topologically and chemically complementary functional groups of the host constituents. Several recent reports have demonstrated that organic-based clathrates can be prepared with various pore topologies, including isolated cages, continuous 1-D pores, 2-D interlamellar galleries, and 3-D porous networks. Clathrates based on metal coordination[2−5] and hydrogen-bonding[6−11] networks exhibit open frameworks with topologies that reflect their metal−ligand coordination environments and arrangement of hydrogen-bonding groups, respectively.

In many cases the structures of organic clathrates mimic those of inorganic zeolites and clays, although molecular host frameworks generally lack structural robustness in the absence of included guests. Organic clathrates also differ from their inorganic counterparts in that their inclusion spaces are inherently more tunable with respect to shape, character, and dimensions, in principle leading to more optimized guest selectivities. The softness of the noncovalent interactions in organic host frameworks also introduces struc-

(1) (a) Atwood, J. L.; Davies, J. E. D.; Vogtle, F. *Comprehensive Supramolecular Chemistry*; Pergammon: New York, 1996; Vol. 6. (b) Bishop, R. *Chem. Soc. Rev.* **1996**, 311−319.
(2) Venkataraman, D.; Lee, S.; Zhang, J.; Moore, J. S. *Nature* **1995**, *371*, 591−593.
(3) Melendez, R. E.; Sharma, C. V. K.; Zaworotko, M. J.; Bauer, C.; Rogers, R. D. *Angew. Chem., Int. Ed. Engl.* **1996**, *35*, 2213−2215.
(4) Aakeröy, C. B.; Nieuwenhuyzen, M. *J. Mol. Struct.* **1996**, *374*, 223−239.
(5) Yaghi, O. M.; Davis, C. E.; Li, G.; Li, H. *J. Am. Chem. Soc.* **1997**, *119*, 2861−2868.
(6) Ermer, O.; Lindenberg, L. *Helv. Chim. Acta* **1991**, *74*, 825−877.
(7) Brunet, P.; Simard, M.; Wuest, J. D. *J. Am. Chem. Soc.* **1997**, *119*, 2737−2738.
(8) Kolotuchin, S. V.; Fenton, E. E.; Wilson, S. R.; Loweth, C. J.; Zimmerman, S. C. *Angew. Chem., Int. Ed. Engl.* **1995**, *34*, 2654-.
(9) Aoyama, Y.; Endo, K.; Anzai, T.; Yamaguchi, Y.; Tomoya, S.; Kobayashi, K.; Kanehisa, N.; Hashimoto, H.; Kai, Y.; Masuda, H. *J. Am. Chem. Soc.* **1996**, *118*, 5562−5571.
(10) Hollingsworth, M. E.; Brown, M. E.; Hillier, A. C.; Santasiero, B. D.; Chaney, J. D. *Science* **1996**, *273*, 1355−1359.
(11) Ramamurthy, V.; Eaton, D. *Chem. Mater.* **1994**, *6*, 1128−1136.

10.1021/cm980600l CCC: $15.00
Published on Web 11/21/1998

tural flexibility that can enable the host to adapt to the steric demands of the guest so that packing can be optimized.

Nevertheless, most organic host frameworks have only a limited ability to adjust to the large differences in steric and electronic demands of various guest molecules while their basic structure is retained. The hydrogen-bonded urea host lattice, which consists of parallel 1-D hexagonal pores that include a variety of linear alkane guests, can adjust slightly through host−guest hydrogen bonding interactions to achieve commensurism with some guests.[12] However, the formation of numerous incommensurate phases and the inability of the 1-D pores to accommodate branched alkanes reflect the resistance of the urea lattice to deformation. Larger guests can be accommodated in the bigger pores of the isostructural thiourea host lattice.[13,14] Recent studies of clathrates based on tri-*o*-thymotide,[15,16] 1:1 anthracene−resorcinol,[17] metal coordination network,[18] and guanidinium arenedisulfonate[19] hosts have demonstrated that, instead of relying on a single architecture conforming to different guest molecules, host frameworks can assume alternative architectures with various porosities to accommodate different guests.

The advancement of clathrates relies on improved understanding of molecular recognition and ensuing host−guest interactions that govern their formation, host architecture, and guest ordering. Guest ordering can depend on very subtle host−guest interactions. For example, isotropically shaped guests such as cyclohexane, chlorocyclohexane, and ferrocene in thiourea host lattices exhibit more disorder than planar guests such as 2,6-diethylnaphthalene and cycloocta-1,5-diene. Perhydrotriphenylene assembles into 1-D hexagonal pores[20] occupied by polar guest molecules with appreciable parallel alignment to generate polar crystals, even though the large distance between guest molecules in neighboring pores (∼15 Å) would argue against interpore guest−guest interactions. However, the extensive disorder of the guest molecules in these structures has precluded a detailed understanding of host−guest interactions that may play a role in long-range ordering of the guests. Rather, the preferential parallel alignment of the guest molecules has been explained in terms of a probabilistic Markov chain model.[21]

Our laboratory recently reported a series of clathrates based on structurally robust, yet flexible, 2-D hydrogen-bonded networks consisting of chemically and topologically complementary guanidinium (G) and sulfonate (S) ions of alkane- and arenedisulfonates organized into either a "quasihexagonal" or "shifted-ribbon" motif.[22,23] The organodisulfonates serve as "pillars" that connect opposing 2-D hydrogen-bonded sheets to create 1-D pores in two-dimensional galleries occupied by guest molecules. The selectivity toward "bilayer" or "brick" lamellar architectures depends on the combined steric requirements of the pillars and guests,[24,25] but the architectures persist, regardless of the pillar or guest structures. The ability to retain the generic 2-D architectures when modifying the host framework by introducing different pillars represents a significant advance in clathrates and provides a route to new inclusion environments with tunable selectivity for a variety of

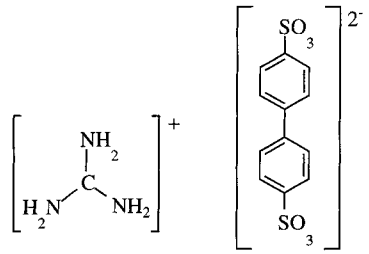

G **BPDS**

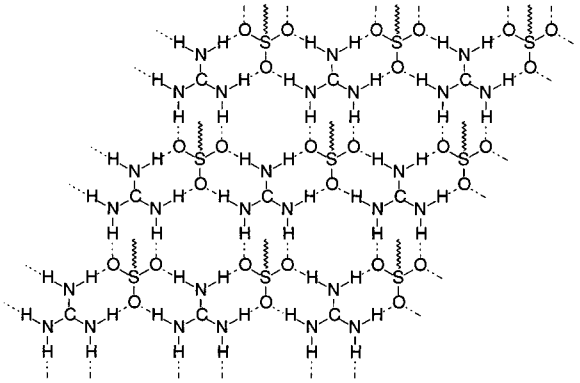

quasihexagonal GS sheet

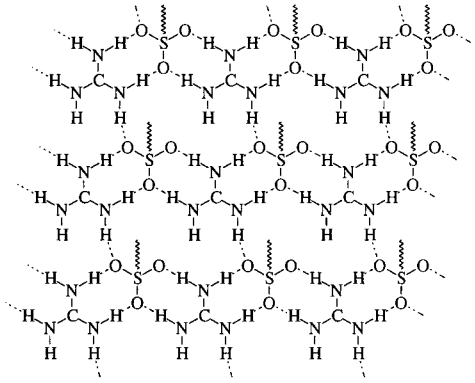

shifted ribbon GS sheet

(12) Brown, M. E.; Chaney, J. D.; Santarsiero, B. D.; Hollingsworth, M. D. *Chem. Mater.* **1996**, *8*, 1588−1591.
(13) Harris, K. D. M. *Chem. Soc. Rev.* **1997**, *26*, 279−289.
(14) Ramamurthy, V.; Eaton, D. *Chem. Mater.* **1994**, *6*, 1128−1136.
(15) (a) Gerdil, R. *Tri-o-Thymotide Clathrates*; Gerdil, R., Ed.; Springer-Verlag: Berlin, 1987; Vol. 140, pp 72−105. (b) Gerdil, R. *Topics Curr. Chem.* **1987**, *140*, 72−105.
(16) Hulliger, J.; Konig, O.; Hoss, R. *Adv. Mater.* **1995**, *7*, 719−721.
(17) Endo, K.; Ezuhara, T.; Koyanagi, M.; Masuda, H.; Aoyama, Y. *J. Am. Chem. Soc.* **1997**, *119*, 499−505.
(18) Hennigar, T. L.; MacQuarrie, D. C.; Losier, P.; Rogers, R. D.; Zarowotko, M. J. *Angew. Chem., Int. Ed. Engl.* **1997**, *36*, 972−973.
(19) Swift, J. A.; Pivovar, A. M.; Reynolds, A. M.; Ward, M. D. *J. Am. Chem. Soc.* **1998**, *120*, 5887.
(20) Hoss, R.; Konig, O.; Kramer-Hoss, V.; Berger, U.; Rogin, P.; Hulliger, J. *Angew. Chem., Int. Ed. Engl.* **1996**, *35*, 1664−1666.
(21) Konig, K.; Burgi, H.-B.; Armbruster, T.; Hulliger, J.; Weber, T. *J. Am. Chem. Soc.* **1997**, *119*, 10632−10640.
(22) Russell, V. A.; Evans, C. C.; Li, W.; Ward, M. D. *Science* **1997**, *276*, 575−579.
(23) Swift, J. A.; Russell, V. A.; Ward, M. D. *Adv. Mater.* **1997**, *9*, 1183−1186.
(24) Swift, J. A.; Pivovar, A. M.; Reynolds, A. M.; Ward, M. D. *J. Am. Chem. Soc.* **1998**, *120*, 5887.
(25) Evans, C. C.; Sukarto, L.; Ward, M. D., manuscript submitted for publication.

Table 1. Crystallographic Data for $(G)_2$BPDS·(guest) Clathrates

compound	1	2	3	4	5
guest	toluene	chlorobenzene	bromobenzene	iodobenzene	*p*-xylene
formula	$C_{21}H_{28}N_6O_6S_2$	$C_{20}H_{25}ClN_6O_6S_2$	$C_{20}H_{25}BrN_6O_6S_2$	$C_{20}H_{25}IN_6O_6S_2$	$C_{22}H_{30}N_6O_6S_2$
FW	524.61	545.03	589.49	636.48	538.64
size (mm^3)	0.50 × 0.18 × 0.08	0.40 × 0.33 × 0.05	0.38 × 0.25 × 0.13	0.24 × 0.11 × 0.08	0.22 × 0.10 × 0.05
color, shape	clear, plate	clear, plate	clear, plate	clear, plate	clear, plate
cryst syst	triclinic	triclinic	triclinic	triclinic	triclinic
space group	$P\bar{1}$ (No. 2)	$P\bar{1}$ (No. 2)	$P\bar{1}$ (No. 2)	$P\bar{1}$ (No. 2)	$P\bar{1}$ (No. 2)
a (Å)	6.1656(1)	6.1605(1)	6.1636(2)	6.1927(3)	6.0964(2)
b (Å)	7.3074(1)	7.2654(2)	7.2688(3)	7.3027(4)	7.3002(2)
c (Å)	14.0760(4)	13.8699(3)	13.9524(6)	14.1951(6)	14.6979(1)
α (deg)	96.898(2)	95.756(1)	96.083(2)	96.825(2)	101.927(1)
β (deg)	93.068(1)	93.969(2)	93.540(1)	92.449(1)	91.077(2)
γ (deg)	92.397(2)	92.532(1)	92.472(2)	92.349(2)	93.525(2)
Z	1	1	1	1	1
vol ($Å^3$)	627.95(2)	615.37(2)	619.61(4)	636.13	638.46(3)
R ($I > 2\sigma$)	0.0359	0.0361	0.0444	0.0589	0.0467
R_w	0.0853	0.0972	0.1129	0.1431	0.101
GOF	1.093	1.05	1.054	0.98	1.039

compound	**6**	**7**	**8**	**9**	**10**
guest	4-chlorotoluene	1,4-dichlorobenzene	4-bromotoluene	1,4-dibromobenzene	*o*-xylene
formula	$C_{21}H_{27Cl}N_6O_6S_2$	$C_{20}H_{24Cl2}N_6O_6S_2$	$C_{21}H_{27Br}N_6O_6S_2$	$C_{20}H_{24Br2}N_6O_6S_2$	$C_{22}H_{30}N_6O_6S_2$
FW	559.06	579.47	603.52	669.39	538.64
size (mm^3)	0.50 × 0.18 × 0.08	0.38 × 0.30 × 0.28	0.28 × 0.06 × 0.05	0.24 × 0.11 × 0.08	0.30 × 0.22 × 0.09
color, shape	clear, plate	clear, plate	clear, plate	clear, plate	clear, plate
cryst syst	triclinic	triclinic	triclinic	monoclinic	triclinic
space group	$P\bar{1}$ (No. 2)	$P\bar{1}$ (No. 2)	$P\bar{1}$ (No. 2)	$P2_1/c$ (No. 14)	$P\bar{1}$ (No. 2)
a (Å)	6.1335(5)	6.1335(5)	6.1150(4)	15.3145(10)	9.1969(1)
b (Å)	7.3803(4)	7.3590(6)	7.3474(4)	7.5637(5)	9.9280(2)
c (Å)	13.8750(8)	13.5867(12)	14.3770(8)	23.903(2)	14.2622(1)
α (deg)	95.007(1)	93.405(2)	98.620(1)	90	83.001(1)
β (deg)	92.148(1)	93.7510(10)	90.193(2)	105.321(1)	83.020(1)
γ (deg)	94.953(1)	95.488(2)	94.611(1)	90	80.443(1)
Z	1	1	1	4	2
vol ($Å^3$)	621.52(6)	607.80(9)	636.50(6)	2670.4(3)	1267.75(3)
R ($I > 2\sigma$)	0.0582	0.0383	0.0574	0.0613	0.0371
R_w	0.1501	0.1021	0.1396	0.1499	0.1006
GOF	1.047	1.021	1.02	1.025	1.053

compound	**11**	**12**	**13**	**14**	**15**
guest	1,2-dichlorobenzene	1,2-dibromobenzene	*m*-xylene	1,3-dichlorobenzene	1,3-dibromobenzene
formula	$C_{20}H_{24Cl2N6}O_6S_2$	$C_{20}H_{24Br2}N_6O_6S_2$	$C_{22}H_{30}N_6O_6S_2$	$C_{20}H_{24Cl2}N_6O_6S_2$	$C_{20}H_{24Br2}N_6O_6S_2$
FW	579.47	669.39	538.64	579.47	669.39
size (mm^3)	0.40 × 0.28 × 0.19	0.40 × 0.20 × 0.12	0.50 × 0.28 × 0.12	0.40 × 0.19 × 0.04	0.35 × 0.21 × 0.12
color, shape	clear, plate	clear, plate	clear, plate	clear, plate	clear, plate
cryst syst	triclinic	triclinic	triclinic	triclinic	triclinic
space group	$P\bar{1}$ (No. 2)	$P\bar{1}$ (No. 2)	$P\bar{1}$ (No. 2)	$P\bar{1}$ (No. 2)	$P\bar{1}$ (No. 2)
a (Å)	7.2825(4)	7.2730(3)	7.2509(2)	6.1882(2)	12.6295(3)
b (Å)	12.3628(7)	12.3595(6)	12.3281(4)	7.1994(2)	14.3458(3)
c (Å)	14.0297(8)	14.0896(6)	29.3761(9)	14.2951(2)	16.0331(4)
α (deg)	91.672(1)	90.569(1)	78.781(1)	98.097(2)	104.108(1)
β (deg)	97.222(1)	98.416(1)	84.872(2)	91.662(1)	110.916(1)
γ (deg)	94.157(1)	94.897(1)	86.372(2)	93.235(1)	92.764(1)
Z	2	2	4	1	4
vol ($Å^3$)	1248.87	1247.99(10)	2562.60(13)	629.07	2602.1(1)
R ($I > 2\sigma$)	0.0503	0.1040	0.0605	0.0482	0.0450
R_w	0.1246	0.2571	0.1422	0.1300	0.0965
GOF	1.019	0.985	1.036	1.042	1.076

differently sized, shaped, and functionalized guest molecules.

We report herein a systematic structural investigation of clathrates constructed from guanidinium cations (G) cations and 4,4′-biphenyldisulfonate (BPDS) anions with various monosubstituted benzene (C_6H_5X; X = Cl, CH_3, Br, I) and disubstituted benzene (*o*,*m*,*p*-YC_6H_5X; X, Y = Cl, CH_3, Br) guests. These $(G)_2$(BPDS)·(guest) structures are refined sufficiently to reveal cooperative host−guest and guest−guest interactions that affect the observed pore structure and guest ordering in the two-dimensional galleries. These materials provide insight into the molecular recognition events that govern the guest ordering in clathrates while demonstrating the adaptability of the flexible $(G)_2$(BPDS) host framework to different guests.

Experimental Section

General Methods. Single crystals of all guanidinium biphenyldisulfonate clathrates, $(G)_2$BPDS·(guest), were grown at room temperature by slow evaporation of saturated methanol solutions containing 2:1 molar ratios of guanidine hydrochloride (Aldrich, 99%), 4,4′-biphenyldisulfonic acid (TCI), and the appropriate aromatic guest. Crystallization solutions typically contained ∼200 mg total of guanidine hydrochloride and 4,4′-biphenyldisulfonate in 5−10 mL of solvent. Clathrates of guests that were solids at room temperature were prepared from solutions containing 1:1 BPDS:guest, whereas an approximately 10−20-fold excess of liquid guests was used (∼1 mL). All guests were used as obtained from commercial sources without further purification [Acros, *o*-xylene (**10**), *m*-xylene (**13**), *p*-xylene (**5**); Sigma, chlorobenzene (99.9%) (**2**), 1,2-dichlorobenzene (99%) (**11**); Aldrich, 1,3-dichlorobenzene (98%) (**14**), 1,4-dichlorobenzene (99%) (**7**), 4-chlorotoluene

(98%) (**6**), bromobenzene (99%) (**3**), 1,2-dibromobenzene (98%) (**12**), 1,3-dibromobenzene (97%) (**15**), 1,4-dibromobenzene (98%) (**9**), 4-bromotoluene (98%) (**8**), iodobenzene (98%) (**4**)]. All single crystals grew as colorless flat plates or thick needles with dimensions of all faces typically exceeding 1 mm^2.

The composition of each clathrate was verified by ^{1}H NMR (DMSO-d_6) solutions prepared from isolated single crystals. ^{1}H NMR spectra were recorded on either a Varian INOVA 500 MHz or a Unity 300 MHz spectrometer. The host lattice constituents were identified by the resonances for the guanidinium ion ($\delta = 6.93$, 12 H, s) and the 4,4′-biphenyldisulfonate ion ($\delta = 7.62-7.70$, 8H, m). The guest identities and stoichiometries were confirmed by their chemical shifts and integrated peak areas.

X-ray Crystallography. Experimental details of the single-crystal X-ray diffraction analyses are provided in Table 1. Single-crystal X-ray structural data were collected on a Siemens SMART Platform CCD diffractometer with graphite-monochromated Mo Kα radiation ($\alpha = 0.71073$ Å) at 173(2) K. Structures were solved by direct methods (SHELXTL-V5.0, Siemens Industrial Automation, Inc., Madison, WI) and refined using full-matrix least-squares/difference Fourier techniques. Absorption corrections were applied with the Siemens Area Detector ABSorption program (SADABS).[26] All non-hydrogen atoms were refined with anisotropic displacement parameters, and all hydrogen atoms were introduced in idealized positions and refined as riding atoms with relative isotropic displacement parameters.

Guest Refinement. Guest molecules **5**, **7**, **10**, **11**, **13**, and **15** were found in fully ordered singly occupied positions within the $(G)_2$(BPDS) host frameworks. Guest molecules **1**−**4**, **6**, **8,** and **14** were disordered between two positions related by an inversion center and were refined with 50% occupancies. Lengthwise librational motion was observed for 4-bromotoluene (**8**). The 1,2-dibromobenzene guests in $(G)_2$(BPDS)·(**12**) were refined with two orientations with a 0.58:0.42 ratio. This occupancy suggested a supercell with 5 times greater volume, but inspection of the crystal structure did not reveal any obvious superstructure. The asymmetric units of $(G)_2$(BPDS)·(**9**) and $(G)_2$(BPDS)·(**15**) each contain two independent guest molecules in which a bromine atom on one of the guests occupies a minor disordered position (0.11 and 0.12, respectively). The structure of $(G)_2$(BPDS)·(**14**) was solved from a crystal with a minor twin component. Structures of $(G)_2$(BPDS)·(**1**), $(G)_2$(BPDS)·(**13**), and $(G)_2$(BPDS)·(**9**) were reported previously.[19,22]

Results and Discussion

The $(G)_2$(BPDS) host framework can adapt to differing steric and electronic requirements of various aromatic guest molecules by several different modes of structural adjustments, including (i) rotation of the (G)N−H···O(S) hydrogen bonds out of the mean plane of the GS sheet with consequential BPDS tilting, (ii) twisting about the central C−C BPDS bond, (iii) rotation about the BPDS C−S bonds, (iv) selecting quasihexagonal or shifted-ribbon hydrogen-bonded motifs in the GS sheet, and (v) selecting "bilayer" vs "brick" stacking motifs. The ability to form clathrates for numerous aromatic guests provides the opportunity to examine systematically the response of the host framework to the guests. The following descriptions of the clathrate structures pertain mainly to modes i−iii, because, with the exception of the 1,4-dibromobenzene clathrate **9**, all adopt the bilayer architecture with the shifted-ribbon motif.

Monosubstituted Aromatic Guests (1−4). The $(G)_2$(BPDS) host framework adopts the bilayer architecture for the monosubstituted aromatic guests **1**−**4**, with the bilayers in the *ab* plane and 1-D pores parallel to the *a* axis. The structure of the chlorobenzene clathrate $(G)_2$(BPDS)·(**2**), illustrated in Figure 1, is representative of hosts containing guests **1**-**4**. The pore *widths* in these clathrates, established by the distance between adjacent pillars along *b*, range from 7.26 to 7.31 Å. The pore *heights*, determined from the minimum separation between the GS sheets at the top and bottom of the 1-D pores (as calculated from the distance between the mean planes of the sheets), range from 10.73 to 11.02 Å (Table 2). As expected, the pore heights decreased with increased tilting of the pillars, with vertical BPDS pillars affording an ideal pore height of 11.2 Å. The coplanar BPDS rings and guest molecules arrange in a herringbone motif, which is common for aromatic molecules.[27,28] The tilts of the guest molecules, as measured by the angle between the axis containing the C−X bond and the normal to the GS sheet, are nearly equivalent for all four clathrates (28.5° ± 2°).

Guests **1**−**4** are disordered between two sites related by an inversion center (Figure 2). Dipole−dipole interactions between guests within a given 1-D pore would be optimized by an antiparallel orientation (...up, down,

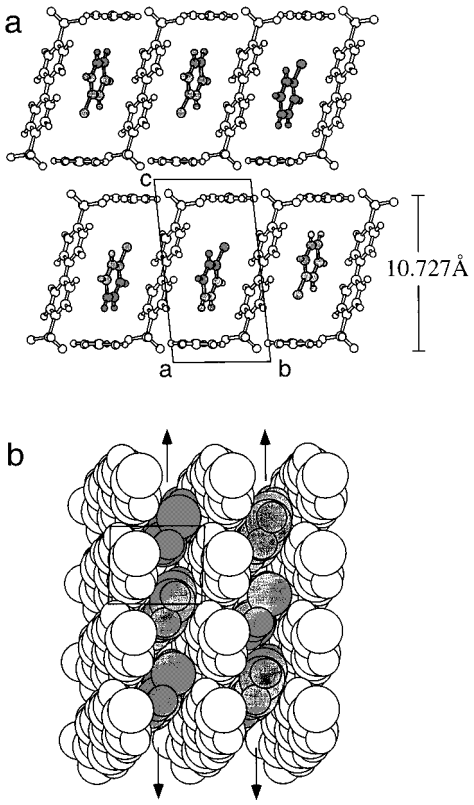

Figure 1. (a) Portions of two bilayers of $(G)_2$(BPDS)·(**2**) as viewed along the pore direction (*a* axis). The chlorobenzene guest molecules (shaded) are disordered about an inversion center. The bilayer height is calculated from the distance between the mean planes of opposing GS sheets. (b) Space-filling representation of the gallery region of $(G)_2$(BPDS)·(**2**) illustrating the herringbone packing of the aromatic rings of the guests and BPDS pillars as viewed along *c**. Guanidinium ions and sulfonate oxygen atoms in the top layer have been removed so that the packing of the guests and pillars can be observed.

(26) Blessing, R. *Acta Crystallogr.* **1995**, *A51*, 33−38.

(27) Desiraju, G. R.; Gavezzotti, A. *J. Chem. Soc. Chem. Commun.* **1989**, 621−623.

(28) Gavezzotti, A. *Chem. Phys. Lett.* **1989**, *161*, 67−72.

Table 2. Summary of Structural Features for $(G)_2$(BPDS)·(guest) Clathrates

	guest	guest volume (Å^3)[a]	PF (without guests)[b]	PF (with guests)[b]	pore direction	BPDS twist	BPDS tilt angle[c]	pore height (Å)	layering
1	toluene	95.39 (0.6)	0.53	0.68	*a*	0	15.07	10.898	bilayer
2	chlorobenzene	93.65 (1.4)	0.55	0.70	*a*	0	16.16	10.727	bilayer
3	bromobenzene	97.87 (2.0)	0.54	0.69	*a*	0	15.69	10.807	bilayer
4	iodobenzene	104.84 (0.5)	0.53	0.69	*a*	0	14.45	11.023	bilayer
5	*p*-xylene	111.78 (1.0)	0.53	0.70	*a*	0	13.94	11.231	bilayer
6	4-chlorotoluene	111.05 (1.0)	0.54	0.71	*a*	0	15.22	10.725	bilayer
7	1,4-dichlorobenzene	108.07 (1.1)	0.55	0.73	*a*	0	17.31	10.473	bilayer
8	4-bromotoluene	113.34 (0.4)	0.52	0.70	*a*	0	12.99	11.088	bilayer
9	1,4-dibromobenzene	117.81 (0.7)	0.50	0.67	*a*	24.6	48		brick
10	*o*-xylene	110.62 (0.6)	0.52	0.70	(110)	19.98	10.93	11.050	bilayer
11	1,2-dichlorobenzene	109.09 (1.1)	0.53	0.71	*b*	0	17.40	10.845	bilayer
12	1,2-dibromobenzene	116.80 (0.2)	0.53	0.72	*b*	0	13.35	10.941	bilayer
13	*m*-xylene	110.92 (0.4)	0.52	0.69	*b*	28.9; 26.01	8.70	11.279	bilayer
14	1,3-dichlorobenzene	107.87 (1.1)	0.53	0.70	*a*	0	13.74	11.087	bilayer
15	1,3-dibromobenzene	117.39 (1.6)	0.51	0.71	*a*	37.77; 30.86	14.76	11.296	bilayer

[a] Calculation based on guest structures determined by X-ray crystallography and by Connolly surfaces using Cerius2 molecular modeling software (version 1.6). [b] PF = packing fraction; calculated using Connolly surfaces using Cerius2. A comparison of arbitrarily chosen examples from the Cambridge Structural Database revealed that the PF values calculated with Cerius2 are systematically lower, by an average of 1.2%, than the Ck values reported by others [see: Kitaigorodskii, A. I. *Molecular Crystals and Molecules;* Academic Press: New York, 1973. Gavezzotti, A. *Nouv. J. Chem.* **1982**, *6*, 443 (1982)}. [c] BPDS tilt angle is the angle between the long axis of BPDS and the normal to the GS mean plane measured along the pore direction. [d] Pore heights were calculated as the distance between the mean plane of opposing GS sheets, neglecting van der Waals radii.

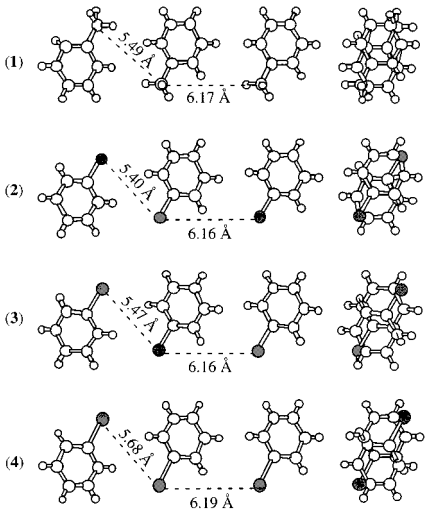

Figure 2. Schematic representation of the ordering of guests **1**−**4** within the 1-D pores of the bilayer $(G)_2$(BPDS) host. As all guests are disordered about two positions related by an inversion center (superposition of orientations at right), the shortest X···X contacts in each of the two possible alignments are noted. Halogen substituents are shaded.

up, down...). However, no such ordering is evident from the crystallographic data for these clathrates. The X···X (X = Cl, Br, I, CH_3) distances (>5.4 Å) between adjacent guests in both possible configurations (up−up and up−down) all exceed the sum of the van der Waals radii,[29] suggesting that, in the case of **2**-**4**, intermolecular halogen−halogen contacts do not significantly influence guest ordering.[30,31] The energy for antiparallel dipole alignment for the monosubstituted guests at the observed intermolecular separations in the 1-D pores is 10−160 times less than kT at room temperature.[32] This indicates that the less favorable parallel alignment of adjacent guests is energetically feasible. Consequently, local disorder about the inversion center, and even dynamic guest rotation, is likely. Dipole−dipole interactions between guests in adjacent pores are expected to be less important than dipole−dipole interactions within the pores, given the increased distance between guests (≈7.3 Å center−center) and dielectric properties of the BPDS pillars.

The guest volumes increase in the order chlorobenzene (**2**) < toluene (**1**) < bromobenzene (**3**) < iodobenzene (**4**). However, the pore heights increase in the order **2** < **3** < **1** < **4** (Figure 3). Sterics appear to be significant for guest organization, as the orientations of the substituents of guests **1**−**4**, with respect to the GS sheets, are nominally identical. The observation of a smaller pore height for **3**, with an attendant decrease in pore volume, as compared to **1**, indicates that steric interactions are not the sole influence on structure. Rather, the shrinking of the pore height upon replacement of the methyl group of **1** with the larger bromo substituent of **3** suggests attractive ion−dipole interactions between the guanidinium ions and the local C−X dipole. Indeed, the closest contacts of guests **1**−**4** with the GS sheets occur through the substituents.[33] The (guest)C−X···GS(host) distances are all well beyond the sum of their van der Waals radii. However, the long-

(29) Pauling, L. *The Nature of the Chemical Bond and the Structure of Molecules and Crystals—An Introduction to Modern Structural Chemistry*; 2nd ed.; Oxford University Press: London, 1940. Cited van der Waals radii are N = 1.5 Å, O = 1.40 Å, Cl = 1.8 Å, Br = 1.95 Å, I = 2.15 Å, CH_3 = 2.0 Å.

(30) Schmidt, G. M. J. *Pure. Appl. Chem.* **1971**, *27*, 647.

(31) Desiraju, G. R. *Organic Solid State Chemistry*; Elsevier: New York, 1987; Vol. 32.

(32) Dipole−dipole energies for parallel alignment were calculated using the equation $w(r,\theta_1\theta_2,\phi) = (u_1u_2)/(4\pi\epsilon\epsilon_0 r^3)[2\cos\theta_1\cos\theta_2 - \sin\theta_1\sin\theta_2\cos\phi]$, where μ_1 and μ_2 are the dipole moments of nearest neighbor molecules, r is the center-to-center intermolecular separation, ϵ and ϵ_0 are the dielectric permittivity ($\epsilon = 8.854 \times 10^{-12}$, $\epsilon_0 = 1$ for intrapore energies and 2.3 for interpore energies mediated by the biphenyl pillars), θ_1 and θ_2 are the angles between neighboring molecular dipoles and the axis connecting the centers of the molecules, and ϕ is the relative azimuthal orientation of the neighboring dipoles aligned parallel ($\phi = 0$). The following are values of $w(r,\theta_1,\theta_2,\phi)$ for intrapore (interpore) interactions in Joules ($\times 10^{22}$): **1**, 0.252 (0.108); **2**, 3.63 (1.92); **3**, 4.08 (2.04); **4**, 5.37 (2.20); **6**, −1.39 (2.36); **8**, 8.18 (−0.154); **10**, 1.63 (0.399); **11**, 26.6 (6.02); **12**, 19.2 (4.23); **13**, −0.873 (0.079); **14**, 21.6 (2.39); **15**, 13.5 (1.21).

(33) Closest C−X···(**G**) contacts measure (**1**) H_3C···C1, 3.764 Å; (**2**) Cl···C7, 3.746 Å; (**3**) Br···N3, 3.779 Å; (**4**) I···N2, 3.774 Å.

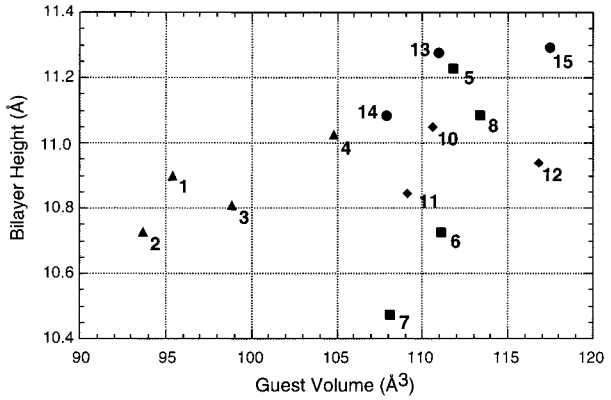

Figure 3. The dependence of bilayer height on guest volumes for bilayer $(G)_2$(BPDS) clathrates for monosubstituted (▲), *o*-disubstituted (◆), *m*-disubstituted (●), and *p*-disubstituted (■) guests, assigned by the numbers in Chart 1.

Chart 1

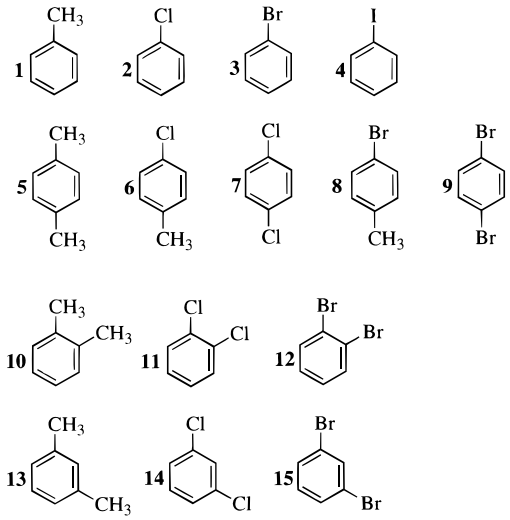

range nature of ion−dipole forces can make these interactions sufficient to cause shrinking of the pore height.

Para-Substituted Guests (5−8). The $(G)_2$(BPDS) clathrates with para-substituted guests **5**−**8** resemble those of the monosubstituted guests **1**−**4**. The coplanar aromatic rings of BPDS pillars flank 1-D pores that are parallel to the crystallographic *a* axis and the tilts of guests **5**−**8**, as defined by the angle between the normal to the GS sheet and the axis containing both substituents, are similar (28.5° ± 2°). The unsymmetrical 4-chlorotoluene (**6**) and 4-bromotoluene (**8**) guests occupy two orientations related by disorder about an inversion center. (Figure 4) Interguest dipolar interactions are apparently not strong enough to enforce local ordering of the unsymmetrical guests within a pore, which is perhaps not surprising given the large separation between guests (ca. 6.1 Å). Furthermore, all intermolecular X···X distances are >5.4 Å, making structure-directing halogen−halogen interactions negligible.

The packing of the pillars and guests in the galleries of $(G)_2$(BPDS)·(**5**) and $(G)_2$(BPDS)·(**7**) is depicted in Figure 5. Despite the similar volumes of methyl and chloro substituents, the BPDS pillars are more tilted and the pore heights are smaller for 1,4-dichlorobenzene

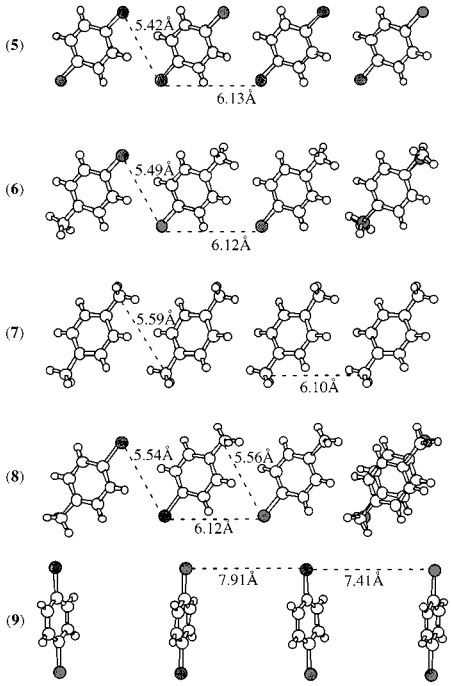

Figure 4. Schematic representation of the ordering of guests **5**−**9** within the 1-D pores of the bilayer $(G)_2$(BPDS) host. Unsymmetrical guests **6** and **8** are disordered about an inversion center, as depicted by the superposition of the disordered molecules at the right. The shortest intermolecular X···X distances are indicated. Halogen substituents are shaded.

(7) than *p*-xylene **(5)**. Pore heights increase in the order 1,4-dichlorobenzene (**7**) < 4-chlorotoluene (**6**) < 4-bromotoluene (**8**) < *p*-xylene (**5**), again differing from expectations based on guest volumes (**7** < **6** < **5** < **8**) and suggesting favorable polar interactions between the halogen substituents and the GS sheets.[34] This is further supported by comparison of the pore height for 1,4-dichlorobenzene (13.52 Å) with chlorobenzene (13.76 Å). The decrease in pore height upon addition of the second halogen substituent argues that attractive host−guest(halogen) interactions play an important role in the structure of these clathrates.

Ortho-Substituted Guests (10−12). As with monosubstituted and para-substituted guests, the pore heights of the clathrates with ortho-substituted benzene guests increase in the order *o*-dichlorobenzene (**11**) < *o*-dibromobenzene (**12**) < *o*-xylene (**10**), differing from the order of the guest volumes (**11** < **10** < **12**).[35] The $(G)_2$(BPDS) host structures for halogenated guests **11** and **12** are quite similar but noticeably different than that of guest **10**. (Figure 6) In $(G)_2$(BPDS)·(**11**) and $(G)_2$(BPDS)·(**12**), the aromatic rings of the BPDS pillars are coplanar and the pore axes are parallel to the crystallographic *b* axis. In contrast, the aromatic rings of the BPDS pillars in $(G)_2$(BPDS)·(**10**) are twisted by 19.98°, and the 1-D pores are parallel to (110). The volumes of the unit cells for clathrates of **10**−**12** are nominally twice that of the clathrates with guests **1**−**8**.

(34) Close X···N(**G**) contacts for **5**−**8** are (**6**) Cl···C7, 3.497 (117.11°), Cl···N3, 3.564 (135.83°), Cl···N2, 3.594 (113.20°); (**7**) Cl···N2, 3.621 (135.28°), Cl···N3, 3.668 (114.27°), H3C···N2, 3.810 (136.13°), H3C···N3, 3.796 (116.07°); (**8**) Br···N2, 3.716 (135.83°), Br···N3, 3.869 (117.87°), Br···C7, 3.715 (119.53°); (**5**) C8···N3, 3.619 (135.01°), C8···C7, 3.635 (125.21°), C8···N2, 3.872 (130.63°).

(35) Closest C−X···(**G**) contacts measure (**11**) Cl1...N2, 3.669 Å; (**12**) Br2···N2, 3.598 Å; Br4...N6, 3.620 Å.

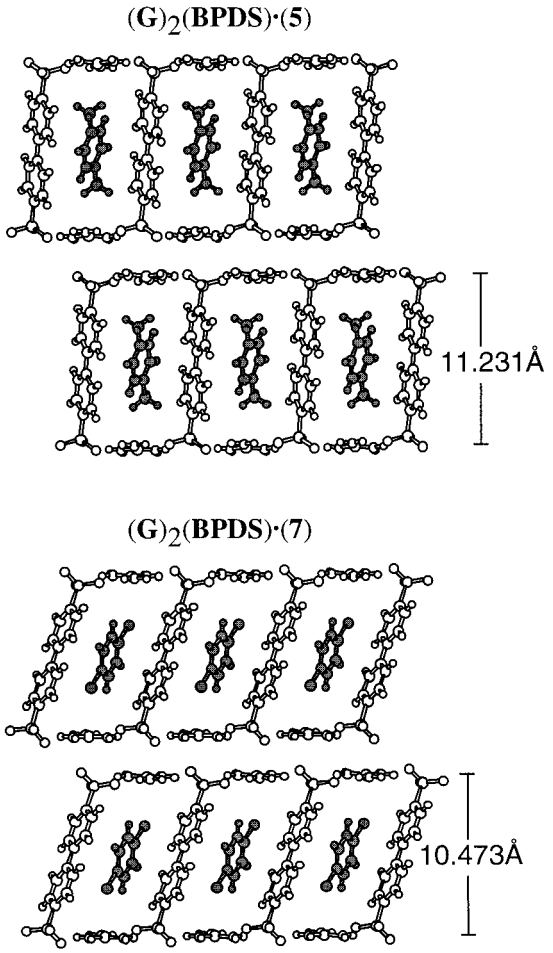

Figure 5. Portions of two bilayers in $(G)_2$(BPDS)·(**5**) and $(G)_2$-(BPDS)·(**7**) as viewed along the pore direction (*a* axis), in which the symmetrical *p*-xylene (**5**) and 1,4-dichlorobenzene (**7**) guests (shaded) occupy fully ordered positions. The bilayer heights differ because of the different tilts of the BPDS pillars.

In the case of **11**, two crystallographically independent guest molecules align antiparallel along a given pore such that adjacent dipoles cancel (Figure 7). Close structure directing Cl···Cl contacts ($d_{Cl\cdots Cl}$ < 4.0 Å) between included guests are not present. The nearest guest molecules in neighboring pores are aligned parallel. While parallel dipole alignment would not be regarded as energetically optimal, the guests in neighboring pores are sufficiently separated (≈7.2 Å) such that dipolar interactions may be subservient to other packing forces.

The asymmetric unit of $(G)_2$(BPDS)·(**12**) was refined with one guest molecule disordered about an inversion center. However, models indicate that these guests must be ordered locally with alternating orientation along the pore, as observed for **11**, in order to avoid implausibly short intermolecular Br···Br contacts (3.3 Å, 0.6 Å shorter than the sum of the van der Waals radii) that would result if the guests were aligned parallel. Antiparallel alignment of adjacent guests about the inversion center results in favorable dipolar interactions while avoiding unreasonably close Br···Br contacts.[36] Therefore, we attribute the guest disorder

(36) Br···Br distances (C−Br···Br angles): Br1···Br1, 5.026 (68.55°); Br2···Br2, 5.561 (60.48°); Br3···Br3, 5.024 (67.74°); Br4···Br4, 5.59 (61.90°).

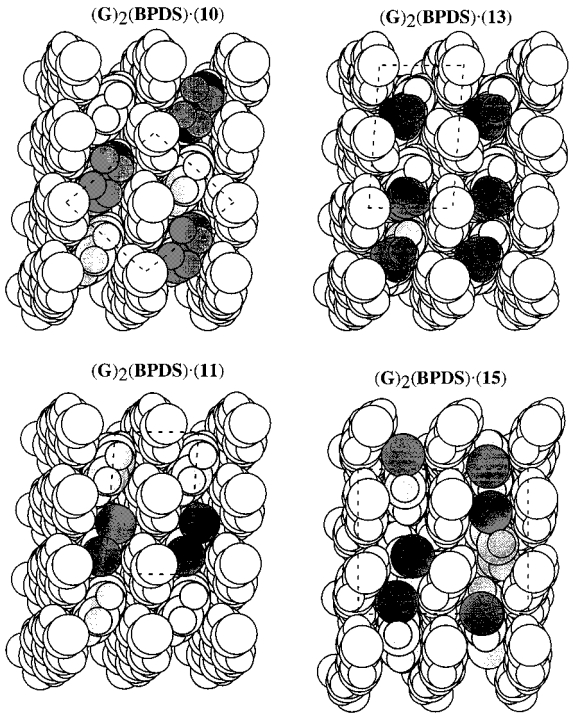

Figure 6. Space-filling representation of the gallery regions of bilayer $(G)_2$(BPDS)·(**10**), $(G)_2$(BPDS)·(**11**), $(G)_2$(BPDS)·(**13**), and $(G)_2$(BPDS)·(**15**) clathrates with *o*-xylene, 1,2-dichlorobenzene, *m*-xylene, and 1,3-dibromobenzene, respectively. Guest molecules are shaded. The Cl, Br, and CH_3 guest substituents are darkened to illustrate both intra- and interpore guest alignment. Guanidinium ions and sulfonate oxygens in the top layer have been removed so that the packing of the guests and pillars can be observed.

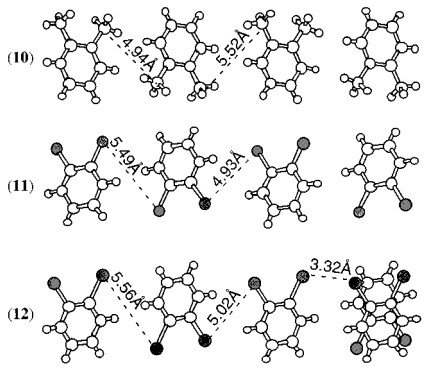

Figure 7. Schematic representation of the ordering of guests **10**−**12** within the 1-D pores of the bilayer $(G)_2$(BPDS) host. The disorder of *o*-dibromobenzene guests (**12**), which is probably artifactual, is depicted on the right. The shortest X···X distances are indicated. Halogen substituents are shaded.

either to rows of guest molecules with alternating orientation offset by a single molecule in adjacent pores or bilayers, or to single site defects capable of shifting the registry of guest molecules within a pore (i.e., ...up, down, (defect), up, down...).

The *o*-xylene molecules in $(G)_2$(BPDS)·(**10**) also are fully ordered within a given pore with alternating orientations, similar to **11** and **12**. However, unlike **11** and **12**, the *o*-xylene guests exhibit antiparallel orientation between nearest neighbors in adjacent pores. This is counter to expectations based solely on dipole moments, as the dipole moment of *o*-xylene is much smaller than that of 1,2-dichlorobenzene (μ(**10**) = 0.62 D; μ(**11**)

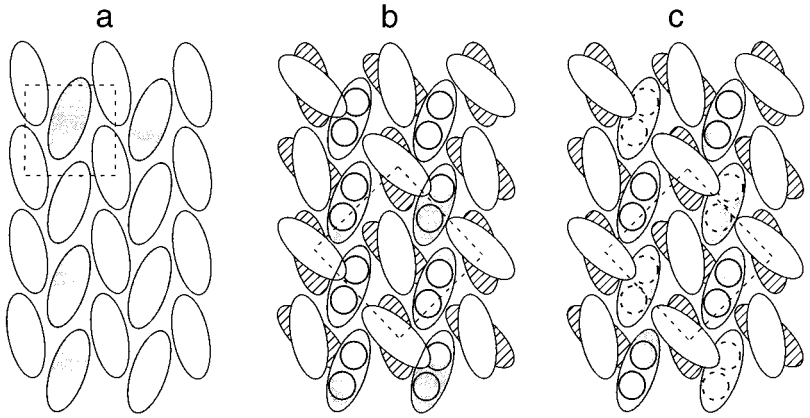

Figure 8. Models illustrating correlated sterically directed host−guest interactions in the galleries of the $(G)_2$(BPDS) bilayer clathrates. The top BPDS aromatic ring (white), bottom BPDS aromatic ring (striped), and guest molecules (gray) are depicted as ovals. Circles with the guest ovals represent the C−X substituents in the "up" (solid circles) or "down" (dashed circles) orientation. (a) Planar BPDS walls with included guests, as observed for monosubstituted and *p*-substituted guests **1**−**8**. In this case, the bottom BPDS ring is not visible because it is eclipsed by the upper ring. (b) A hypothetical model based on the host framework of clathrate $(G)_2$(BPDS)·(**10**), in which the BPDS rings have a conformational twist of ≈20° and all the guests are oriented with the *o*-substituents "up". Every other guest molecule in the pore experiences an unfavorable steric interaction with the upper ring of the BPDS pillar (symmetry dictates identical effects with the *o*-substituents "down"). (c) A model of the guest ordering observed for $(G)_2$(BPDS)·(**10**), in which the guest orientation alternates along the pore (...up, down, up, down...) so that unfavorable steric interactions between the BPDS rings and the halogen substituents are avoided. The observation of antiparallel interpore guest orientation for **10**, but a parallel alignment for **11** and **12**, indicates that the twist of the BPDS rings in $(G)_2$(BPDS)·(**10**) acts as a "gearing" mechanism that enforces the antiparallel orientation.

= 2.50 D). This observation suggests that interpore ordering is directed by correlated steric effects rather than by dipolar interactions.

The role of sterics in guest ordering can be illustrated by the simple geometric model of the occupied galleries illustrated in Figure 8, in which the upper BPDS aromatic rings are depicted as white ovals, the lower BPDS aromatic rings as striped ovals, and the guest molecules as gray ovals. The halogen and methyl substituents of the guests are depicted as circles, with solid and dashed outlines representing "up" and "down" orientations, respectively. In case a, the aromatic rings of the BPDS pillar are coplanar so that the upper BPDS rings eclipse the lower ones, and the orientation and alignment of the guest molecules are unspecified. Ignoring the effect of any guest−guest interactions, there are no guest−host steric interactions that would direct the guest molecules into "up" or "down" orientations, as both orientations would experience the same steric environment with the upper and lower BPDS ring. Model a, therefore, describes $(G)_2$(BPDS)·(guest) clathrates with coplanar BPDS pillars in which there is no correlated ordering between guests in adjacent pores (**1**−**8**).

In contrast, conformational twisting of the BPDS pillars introduces steric effects that can result in correlated guest ordering. The schematic representation in Figure 8b of $(G)_2$(BPDS)·(**10**), for which the BPDS rings exhibit a conformational twist of 20°, illustrates this effect. Every other guest molecule within a pore experiences an unfavorable steric interaction between the ortho substituents and the upper BPDS ring if all the guests are oriented "up" (the same steric effect occurs with the lower BPDS ring if the guests are all oriented "down"). If the guest orientation alternates (...up, down, up, down...) along the pore, these unfavorable steric interactions are avoided, as depicted in Figure 8c. Notably, pillars flanking a guest on opposite sides of the pore are related by inversion, forcing the guest in the next pore to choose the opposite orientation to avoid the same unfavorable steric interactions. Therefore, the conformationally flexible BPDS pillars behave as *synchronized molecular gears* that relay information for pore-to-pore guest ordering during assembly of the galleries.

Meta-Substituted Guests (13−15). Unlike the aforementioned examples, $(G)_2$(BPDS) clathrates of the meta-substituted guests **13**−**15** exhibit an increase in the pore heights that parallels the guest volume (1,3-diclorobenzene (**14**) < *m*-xylene (**13**) < 1,3-dibromobenzene (**15**)). However, there are noticeable differences among the clathrates with respect to both the host framework and guest−guest organization within the pores. The asymmetric units of $(G)_2$(BPDS)·(**13**) and $(G)_2$(BPDS)·(**15**) each consist of two independent guest molecules, two independent BPDS ions, and four guanidinium ions. The clathrate of **13** has 1-D pores, parallel to the crystallographic *b* axis, flanked by the two independent BPDS pillars with conformational twists of 28.9° and 26.0° (Figure 6). The clathrate of **15** has 1-D pores, parallel to the *a* axis, flanked by two independent BPDS pillars with twists of 30.86° and 37.77°. The clathrate of **14** has 1-D pores parallel to the *a* axis, flanked by coplanar BPDS pillars and occupied by *m*-dichlorobenzene guests.

Interguest alignment within the pores of these inclusion compounds is also markedly different (Figure 9). Guest molecules in $(G)_2$(BPDS)·(**13**) are close-packed head-to-tail along a given pore, reminiscent of the crystal structures of many pure meta-substituted aromatics.[37] Within a given bilayer, the head-to-tail guest chains are aligned in the same direction, but the guests are aligned antiparallel in adjacent bilayers, as required by centrosymmetry. We attribute the long-range interpore guest ordering within a bilayer in $(G)_2$(BPDS)·(**13**) and $(G)_2$(BPDS)·(**15**) to correlated guest−host−guest

(37) Curtin, D. Y.; Paul, I. C. *Chem. Rev.* **1981**, *81*, 525−541.

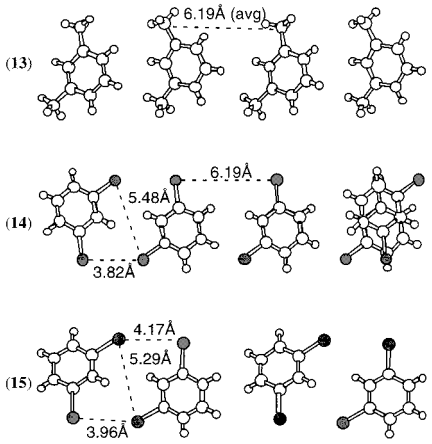

Figure 9. Schematic representation of the ordering of guests **13**−**15** within the 1-D pores of the bilayer $(G)_2$(BPDS) host. The shortest X···X are indicated. The observed disorder of guest **14** is depicted at the right. Halogen substituents are shaded.

steric interactions similar to those described for the *o*-xylene clathrate. Illustrating this effect is difficult owing to the existence of two independent BPDS pillars with different conformations, but analysis of the crystal structure reveals that a similar gearing mechanism is likely responsible for the ordering.

The two independent *m*-dibromobenzene guests in $(G)_2$(BPDS)·(**15**) are fully ordered, alternating their alignment along a pore, and exhibiting interguest Br···Br contacts that are only 0.06 Å longer than the sum of their van der Waals radii.[38] This suggests a role for Br···Br interactions in the guest ordering, in this case resulting in the formation of dimerized "superguests" that are inherently nonpolar. The bromine substituents also exhibit several close contacts of <3.6 Å with the GS sheets that suggest ion−dipole interactions.[39]

The guest orientations of **14** and **15** within a given pore are nominally identical, but the *m*-dichlorobenzene guests in $(G)_2$(BPDS)·(**14**) are disordered with 50% occupancy about an inversion center. The observed disorder of **14** may be artifactual, resulting from rows of *ordered* guests that are offset in adjacent pores by *a*/2. The shortest Cl···Cl contacts between neighboring guests molecules in a pore are 3.82 Å,[40] which is 0.22 Å larger than the sum of the van der Waals radii (3.6 Å). It is reasonable to suggest that these X···X interactions prevent disorder of **15**, whereas disorder of **14** is more likely owing to the coplanar BPDS rings and larger interguest separation, which reduces the structure-directing influence of the Cl···Cl interactions.

The Exception to the Bilayer Motif: $(G)_2$(BPDS)·(9). Among this series of $(G)_2$(BPDS)·(guest) clathrates, $(G)_2$(BPDS)·(**9**) has a truly unique host architecture, crystallizing in a compositionally identical "brick" form in which pillars project from both sides of a given GS sheet so that all GS sheets are continuously connected (Figure 10).[20] This demonstrates an additional mode by

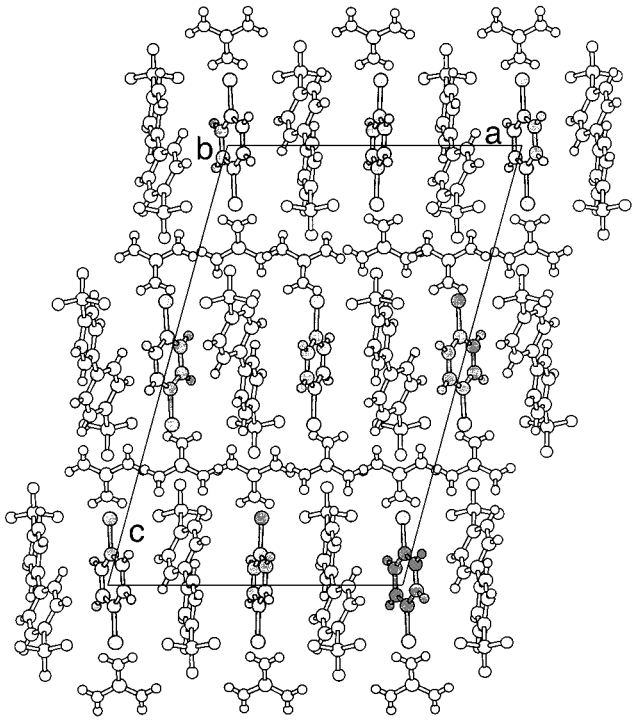

Figure 10. Packing diagram of $(G)_2$(BPDS)·(**9**) viewed along the *a* axis. Guest molecules are shaded.

which the GS-based hosts can adapt to different guests, in this case by forming an architecture with nominally twice the porosity that retains the lamellar organization imposed by the 2-D GS sheet. The brick framework, which is capable of puckering, is inherently more flexible than the bilayer form, for which puckering is sterically prohibited. Puckering of the brick framework, accompanied by tilting of the BPDS pillars, decreases the actual pore dimensions. This capability allows the brick framework to conform to guests such as **9** that are not large enough to occupy the voids of an ideal brick framework in which the BPDS pillars are vertical. The 1-D pores in $(G)_2$(BPDS)·(**9**), which are orthogonal to the direction of the GS ribbons and flanked by twisted BPDS pillars, are occupied by the 1,4-dibromobenzene guests. The C−Br bonds of the guests project into pockets formed by corrugation of the GS sheets, resulting in ion−dipole interactions between the bromine substituents and the GS.[41] Consequently, the switch to the brick isomer in the presence of **9** can be attributed to the increased steric demands of this guest relative to the others combined with the capacity of the clathrate to achieve favorable polar interactions by puckering of the GS network around the guests.

Conclusion

The solid-state structures of the bilayer $(G)_2$(BPDS)·(guest) clathrates suggest that the guest ordering in the 2-D galleries is influenced largely by cooperative steric interactions between the rotationally and conformationally flexible BPDS pillars and the guest molecules. The BPDS pillars behave as synchronous molecular gears that relay the instructions for guest ordering from one pore to another, either by rotating about the (sul-

(38) Br1···Br3, 3.96 Å; C−Br···Br1, 143.5°; C−Br1···Br3 92.8°; Br2···Br4,4.17 Å; C−Br2...Br4, 137.9°; C−Br4···Br2, 87.4°.

(39) Br1···N3, 3.49 Å; Br1···C25, 3.55 Å; Br1···N2, 3.89 Å; Br4···N10, 3.51 Å; Br4···C28, 3.65 Å.

(40) C−C12···Cl1 and C−C11···Cl2 angles are 132.12° and 95.94°, respectively.

(41) Br1...N3(G), 3.48 Å; Br2...N5(G), 3.57 Å.

fonate)S−C(phenyl) bond or by conformational twisting about the central C−C bond of the BPDS pillar. These steric effects can induce guest ordering that is less than optimal with respect to guest−guest dipolar interactions. The flexibility of the $(G)_2$(BPDS) host framework is further demonstrated by its ability to contract with the introduction of halogen substituents in order to exploit polar host−guest interactions between the halogen substituents and the ionic GS sheets. The ability of the host framework to relax about different guest molecules with a diverse set of steric demands and substitution patterns reveals a robustness that is quite extraordinary. This characteristic is crucial for elucidating the physicochemical basis for molecular recognition associated with subtle host−guest interactions in organic clathrates. It is possible that similar effects may influence long-range guest ordering in other clathrates, including polar inclusion compounds such as perhydrotriphenylene.

Acknowledgment. The authors gratefully acknowledge the assistance of Victor G. Young, Jr. of the X-ray Crystallographic Laboratory at the University of Minnesota. This work was supported by the National Science Foundation. A.M.R. acknowledges financial support from the National Science Foundation Research and Education Undergraduate Program. We thank Wenjie Li for providing single crystals of $(G)_2$(BPDS)·(**1**) and $(G)_2$(BPDS)·(**13**).

Supporting Information Available: Tables of X-ray data collection/refinement parameters, atomic position parameters, anisotropic displacement parameters and thermal ellipsoid plots for $(G)_2$(BPDS) containing guests **2**−**8, 10**−**12, 14** and **15** (86 pages); observed and calculated structure factors (88 pages). Ordering information is given on any current masthead page.

CM980600L